# The photocatalytic activity of sol-gel derived photo-platinized TiO2 films

Cyril Millon, David Riassetto, Grégory Berthomé, Francine Roussel, Michel Langlet

# The photocatalytic activity of sol–gel derived photo-platinized $TiO_2$ films

C. Millon [a], D. Riassetto [a], G. Berthomé [b], F. Roussel [c], M. Langlet [a,*]

[a] *Laboratoire de Matériaux et de Génie Physique, INPG-MINATEC, 3 parvis Louis Néel, BP 257, 38016 Grenoble Cedex 1, France*
[b] *Laboratoire de Thermodynamique et de Physico-Chimie Métallurgique, ENSEEG-INPG, BP 75, Domaine Universitaire, 38402 Saint Martin d'Hères, France*
[c] *Consortium des Moyens Technologiques Communs, ENSEEG-INPG, BP 75, Domaine Universitaire, 38402 Saint Martin d'Hères, France*

Sol–gel $TiO_2$ thin films have been loaded with platinum clusters through a photo-platinization method using water/ethanol platinum solutions. The morphological and physico-chemical properties of platinized films as well as the chemical state of platinum clusters have been studied by scanning electron microscopy, Fourier transform infrared spectroscopy, and X-ray photoelectron spectroscopy. These characterizations show that morphological and physico-chemical properties are strongly influenced by the water/ethanol composition of the platinum solution and temperature of the post-platinization heat-treatment, which in turn determines the photocatalytic performances of platinized films. UV-assisted photocatalytic reactions induced by platinized films follow bi-regime kinetics. The first regime is characterized by a rather high rate constant, while long term UV exposition promotes a more or less pronounced deceleration of the photocatalytic reaction. Optimization of the photocatalytic activity requires a platinization in presence of a water excess followed by a heat-treatment in the 250–400 °C thermal range. Films processed in such conditions exhibit rate constants in the first and second photocatalysis regime which are four times and three times greater, respectively, than the rate constant measured for non-platinized films.

*Keywords:* Photocatalytic activity; Sol–gel thin films; Titanium oxide; Platinum clusters

## 1. Introduction

Over the three past decades, platinized $TiO_2$ photocatalysts have been the object of tremendous interest. Though the exact electronic nature of the Pt–$TiO_2$ contact is still matter to controversy, it has generally been reported that surface loading of $TiO_2$ particles with small platinum clusters greatly improves the photocatalytic properties of titanium oxide. In the early eighties, using a concept introduced by Nozik [1], Sakata et al. have discussed the photocatalytic properties of Pt loaded $TiO_2$ particles in terms of photo-chemical diode [2]. This model involves the formation of a Schottky barrier at the metal-semiconductor interface, with creation of an electron depletion layer at the Pt–$TiO_2$ junction and bending down of the $TiO_2$ conduction and valence bands. The Schottky barrier is generally referred to in the literature to explain the beneficial effect of Pt clusters on the $TiO_2$ photocatalytic activity. Owing to this barrier, photo-electrons $e^-$ generated under UV light in the n-type $TiO_2$ semiconductor are readily transferred to and trapped in Pt nanoparticles, while photo-holes $p^+$ are directed towards the semiconductor surface. This feature allows an efficient separation of photo-generated charge carriers, *i.e.* efficiently prevents an $e^-/p^+$ recombination, which greatly improves the photoactivity. Under UV illumination, the Pt Fermi level and $TiO_2$ band bending are imposed by the light intensity, which globally determines the charge carrier generation and separation efficiencies together with efficiency of charge carrier transfer towards the electrolyte, *i.e.* the matter to be photocatalytically decomposed. Thus, based on the photochemical diode model, anodic oxidation and cathodic reduction reactions occurring under

* Corresponding author. Tel.: +33 4 56 52 93 22; fax: +33 4 56 52 93 01.
*E-mail address:* Michel.Langlet@inpg.fr (M. Langlet).

UV light separately take place at the $TiO_2$ and metal surface, respectively.

Improved performances of Pt–$TiO_2$ photocatalysts rely on several factors, including size, distribution, amount, or chemical state of Pt clusters. Ohtani et al. have pointed out that an optimal Pt loading value together with an homogeneous distribution of Pt clusters at the $TiO_2$ particle surface are required to enhance the photocatalytic activity [3]. In their experimental conditions, these authors determined an optimal average distance between Pt clusters of *ca.* 10 nm. The authors also showed that excess loading of Pt reduced the photocatalytic rate owing to a decrease in light absorption by $TiO_2$ and enhanced recombination of photo-generated electron–hole pairs. Sadeghi et al. have indicated the essential role of number and size of Pt clusters [4]. They have confirmed that, as the number of Pt clusters increases, *i.e.* for a too heavy Pt loading, metal particles act as recombination centres for photo-generated electrons and holes. Furthermore, the Pt cluster size can influence the Fermi level of the metal, which in turn affects the $TiO_2$ to Pt and/or Pt to electrolyte transfer of electrons and the related electron–hole separation. In their experimental conditions, Sadeghi et al. determined an optimal Pt cluster size and loading yield of 2 nm and 2 wt%, respectively. Gan et al. have also reported that too small Pt clusters loose their metallic character, which strongly modifies their catalytic activity [5]. Such a metallic to non-metallic transition was evidenced for clusters below 2 nm in diameter. Platinization features, *i.e.* size, distribution, amount, or chemical state of Pt clusters, greatly depend on the procedure used for loading $TiO_2$ particles with platinum. Among the numerous thermo-, chemico-, or photo-induced reduction methods used for loading metallic Pt clusters, photo-metallization is one of the most investigated [4,6–11]. This versatile method, which was introduced at the end of the seventies, is generally considered to yield more active photocatalysts than other methods [9], and it has been adapted to many noble metals including Pt, Pd, Ru, Rh, or Ag [6,10,11]. In particular, it does not require any thermal treatment under reducing atmosphere that might modify the $TiO_2$ support. Photo-platinization involves adsorption at the $TiO_2$ surface of a $Pt^{4+}$ precursor, generally chloroplatinic acid in aqueous solution, followed by reduction of $Pt^{4+}$ cations by electrons photo-generated in the $TiO_2$ conduction band under UV irradiation. The anodic process is the oxidation of water by valence band photo-holes. Furthermore, a sacrificial oxidizable additive, *e.g.* an alcohol, is usually added in the aqueous solution. It acts as a sacrificial electron donor/hole scavenger and favours a better photo-generated charge carrier separation, thus promoting a greater photo-metallization rate.

Up to now, the photo-platinization method has essentially been applied to $TiO_2$ photocatalytic powders intended for unsupported photocatalyst or ceramic photocatalyst applications. When titanium oxide is immobilized on a rigid support in the form of a thin film, new photocatalytic applications can be envisaged that have been largely investigated over the past decade, including supported photocatalysts for water purification [12], antibacterial surfaces [13], photo-active surfaces for deodorizing or purifying indoor atmospheres [14], or self-cleaning surfaces [15]. It is surprising to note that, despite well recognized benefits of platinum clusters loaded at the surface of a $TiO_2$ photocatalyst, surface platinization of $TiO_2$ thin films has rarely been investigated for photocatalytic applications. Recently, Zhang et al. have proposed a chemically modified method for loading Pt clusters at the surface of $TiO_2$ films [16,17]. They reported that, under oxidizing atmosphere, platinum could thermally diffuse into the films upon heating at 400 °C, leading to an interstitial or substitutional $TiO_2$ doping. Some recent works have been devoted to the photo-platinization of $TiO_2$ thin films. He et al. reported on enhanced catalytic decomposition of formic acid at the surface of photo-platinized $TiO_2$ films [18]. They mentioned that decomposition not only arose from a photocatalytic effect but also from a purely catalytic effect induced by holes in the Pt d-band. Such a dual effect was also reported by other authors [7]. Kim et al. reported on enhanced photocatalytic properties of photo-platinized $TiO_2$ films using benzene as a model molecule to be photocatalytically decomposed [19]. They pointed out the necessity of a small Pt amount for obtaining optimal photocatalytic properties of platinized films. These works prove that the photo-platinization method can be extrapolated to photocatalytic thin films and Pt–$TiO_2$ interfacial effects can promote an enhanced photo-activity of platinized films.

However, to the best of our knowledge, the literature is by far insufficient to determine what should be optimum photo-platinization conditions yielding best photocatalytic properties of Pt–$TiO_2$ films and to which extent these properties can be enhanced by Pt–$TiO_2$ interface effects. In particular, few is known on how the photocatalytic activity of photo-platinized $TiO_2$ films is influenced by the Pt solution formulation, the presence and nature of an oxidizable additive in the Pt solution, irradiation conditions during platinization, post-platinization heat-treatment conditions, etc.. . . Furthermore, numerous data cited in the literature devoted to photo-platinized powders can hardly be employed to infer optimum film photo-platinization conditions. It arises from two main reasons. Firstly, photocatalytic characterizations of platinized powders mentioned in the literature are generally performed using very distinct methods (nature of the model molecule to be decomposed, oxidative or reductive decomposition procedures, gas or liquid phase photodecomposition), which reduces possibilities of making objective comparisons and drawing conclusions on ideal platinization conditions. Besides, results on platinized powdered photocatalysts cannot directly be extrapolated to thin film photocatalysts because involved mechanisms are somewhat different. In particular, our previous works suggest that, compared to powdered photocatalysts, thin film photocatalysts undergo a greater probability of $e^-/p^+$ recombination [20–22]. It can therefore be inferred that platinization criteria required for efficiently preventing charge carrier recombination should noticeably differ for film and powdered catalysts. In this context, a specific research on photo-platinized films remains of academic and technologic interest. In this paper, we present new studies performed on photo-platinized $TiO_2$ sol–gel thin films. We particularly focus on influence of the Pt solution formulation, photo-platinization duration, and post-platinization heat-treatment. These parameters are tested with respect to the photocatalytic activities of

Pt–$TiO_2$ films in relation to their physico-chemical and morphological properties.

## 2. Experimental

### 2.1. $TiO_2$ sol and film preparations

$TiO_2$ films were deposited from a polymeric sol, which was prepared by mixing tetraisopropyl orthotitanate (TIPT; $Ti(C_3H_7O)_4$ from Fluka) with deionised water, hydrochloric acid, and absolute ethanol as a solvent. TIPT concentration in the solution was fixed at 0.4 M, and the TIPT/$H_2O$/HCl molar composition was 1/0.82/0.13. The sol was aged at room temperature for 2 days before first depositions, after what it could be used for several weeks in reproducible deposition conditions. Films were deposited at room temperature on (1 0 0) silicon wafers ($3.3 \times 3.3\,cm^2$) by spin-coating using a Suss Microtec RC8 apparatus. Prior to deposition, the substrates were cleaned with ethanol, then rinsed with deionised water, and dried with air spray. For each deposition, 300 μL of sol were spread on the substrate rotated at 3000 rpm. After liquid film deposition, the solvent rapidly evaporated and a solid film formed at ambient atmosphere through the well-known sol–gel polymerization route. A Multi-layer procedure was adopted to fix the final oxide film thickness at around 250 nm. Each as-deposited single-layer film was heat-treated in air for 2 min at 500 °C before deposition of a subsequent single-layer. The final 7-layer film was then heat-treated at 500 °C for 2 h. Our previous works showed that such conditions yielded well crystallized anatase $TiO_2$ films with good photocatalytic activity [21,22].

### 2.2. Photo-platinization conditions

Photo-platinization experiments were performed using chloroplatinic acid hexahydrate ($H_2PtCl_6{\cdot}6H_2O$ from Strem Chemicals) in aqueous solution. The chloroplatinic acid concentration was fixed at 0.2 mM. Absolute ethanol was used as a sacrificial oxidizable additive. The water/ethanol molar ratios were initially fixed at 0/100, 50/50, 80/20, or 100/0. However, during preliminary photo-platinization tests, we observed a precipitation for the latter formulation, which rapidly occurred under UV exposition. In this paper, we will thus focus on the three former formulations, for which any precipitation could not be observed over the whole duration of photo-platinization experiments. For those experiments, titania films were settled in a glass photoreactor opened to air containing a volume of 100 cc of the chloroplatinic acid solution. The photoreactor was installed in a climatic cabinet regulated at a 20 °C temperature and 40% relative humidity. Constant agitation of the solution was insured using a magnetic stirrer. Before UV-irradiation, the solution was first stored in the dark for 60 min to reach equilibrated adsorption of chloroplatinic acid at the film surface. $TiO_2$ films were then exposed for various durations, ranging up to 14 h, to UV radiation provided by three Philips PL-S 11 UV-lamps. These lamps only emit in the UVA spectral range (negligible UVB/UVC emission) with a maximal emission at 365 nm. An overall UV light intensity of around $30\,mW/cm^2$ was measured at the film surface. After photo-platinization, the films were heat-treated in air for 2 h at various temperatures ranging from 110 to 500 °C. In this article, platinized films are nomenclatured with respect to the water/ethanol molar composition of the Pt solution, *e.g.* 80/20 films were platinized from a 80/20 water/ethanol solution.

### 2.3. Film characterizations

Physico-chemical and morphological properties of platinized $TiO_2$ films were analyzed using various techniques. A Philips XL 30 scanning electron microscope (SEM) operated at 10 kV was employed for energy dispersive X-ray (EDX) analyses. Surface imaging was performed using a ZEISS Ultra 55 Field Emission Gun (FEG)-SEM operated at 4 kV. Fourier transform infrared (FTIR) spectra were collected in transmission, in the 4000–250 $cm^{-1}$ spectral range with a resolution of 4 $cm^{-1}$, using a Bio-Rad FTS-165 spectrometer. Spectra corresponding to 300 scans were recorded in room atmosphere after purging the measurement chamber with dry air for 15 min. The spectra were analyzed after subtraction of the bare substrate spectrum. Surface chemical analysis was performed by X-ray photoelectron spectroscopy (XPS) using a XR3E2 apparatus from Vacuum Generator employing an Mg Kα source (1253.6 eV). Before collecting data, the samples were put in equilibrium for 24 h in an ultra high vacuum chamber ($10^{-10}$ mbar). Photoelectrons were collected by a hemispherical analyzer at 30° and 90° take-off angles. The spectra were calibrated with the C1s peak at 284.7 eV. They were analyzed in the Pt4f region. For that purpose, the $Pt4f_{7/2}$:$Pt4f_{5/2}$ doublets were deconvoluted using a least-square curve fitting program based on a mixed Gaussian/Lorentzian function, which accounted for the peak asymmetry, and assuming a 4:3 intensity ratio of the doublet components and a splitting energy of 3.3 eV.

Photocatalytic properties of platinized films were studied through the oxidative photo-decomposition of Orange G (OG; $C_{16}H_{10}N_2Na_2O_7S_2$ from Aldrich) in aqueous solution (25 mg/L; 100 cc) using the same device as that used for photo-platinization experiments. Before UV-irradiation, the solution was first stored in the dark for 60 min to reach equilibrated adsorption of OG at the film surface, after what the film was exposed for 3 h to UV-irradiation under magnetic stirring. Small solution aliquots were periodically withdrawn in order to measure the concentration variations of OG as a function of irradiation time. Transmission spectra of liquid samples were collected in the 300–600 nm spectral range using a Jasco V-530 spectrophotometer. OG concentration variations were deduced from absorbance variations of the main OG absorption band at 480 nm. The photocatalytic activity was determined from the rate of disappearance of OG by plotting $\ln(C_0/C)$ as a function of the irradiation time $t_{UV}$, where $C_0$ and $C$ account for the OG concentration before and after exposition, respectively. Blank UV irradiations performed for 3 h without titania films did not allow to detect any variation of the OG concentration, which indicated that no photolysis occurred over the whole duration of the photocatalytic experiments. Besides, negligible variations of the OG concentration observed after storage of platinized film

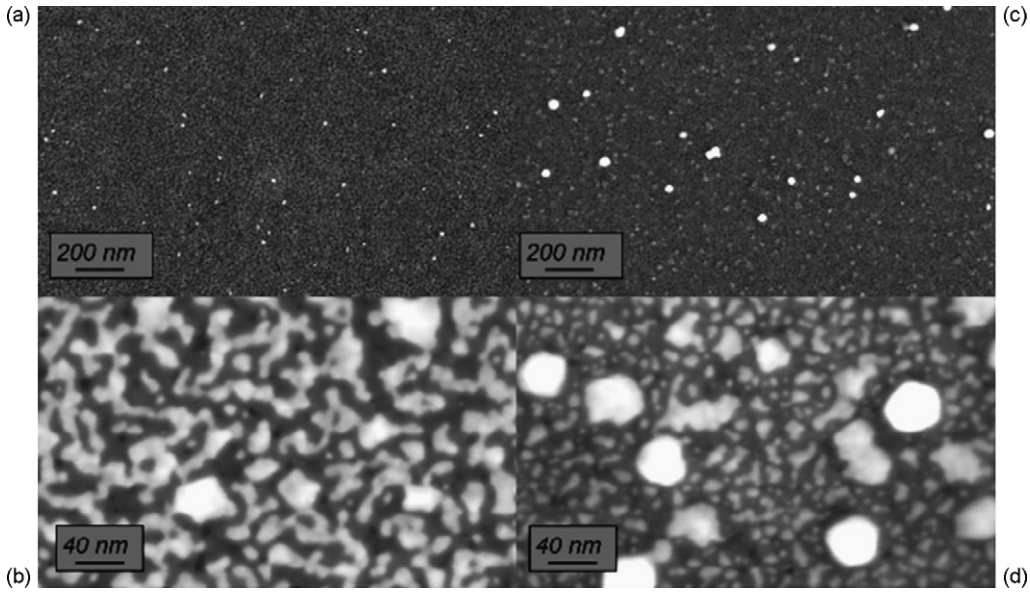


Fig. 1. FEG-SEM images of 0/100 films platinized for (a) 60 min and (b) 14 h, and 80/20 films platinized for (c) 120 min and (d) 14 h.

in the dark for 60 min indicated that, in our experimental conditions, any catalytic (non-photocatalytic) mechanism induced by platinum particles did not significantly participate in the OG decomposition. Both observations allow concluding that photodecomposition features described in following sections only arise from pure photocatalytic effects.

## 3. Results and discussion

### *3.1. Photo-platinization features*

FEG-SEM imaging and EDX analysis were used to study the influence of the photo-platinization duration and composition of the chloroplatinic solution on the amount and morphology of platinum clusters loaded from 0/100 and 80/20 water/ethanol solutions. For both solutions, *Z*-contrasts in FEG-SEM images of Figs. 1 and 2 clearly evidence the presence of Pt clusters, which appear as white spots distributed on the $TiO_2$ film surface. In the high magnification images of Fig. 2, $TiO_2$ grain boundaries can also be appreciated. For short platinization durations, high magnification images of Fig. 2 and weaker magnification images of Fig. 1a and c indicate a broad distribution of cluster sizes that range from less than 5 nm to about 50 nm. The size of smallest clusters could not be precisely determined owing to limitations in the FEG-SEM sensitivity. Figs. 1 and 2 also show that, compared to a 100% ethanol solution, a water-rich solution yields larger clusters and a weaker amount of small clusters, *i.e.* the cluster size distribution is shifted toward larger values. In the previous

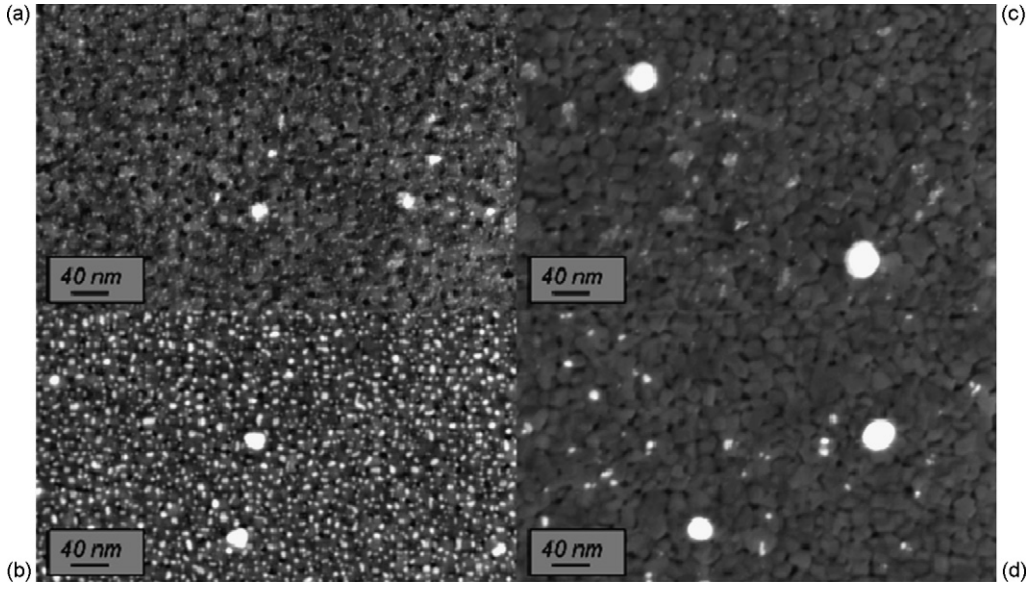


Fig. 2. FEG-SEM images of 0/100 films platinized for 60 min and subsequently heat-treated at (a) 110 °C and (b) 500 °C, and 80/20 films platinized for 120 min and subsequently heat-treated at (c) 110 °C and (d) 500 °C.

section, we indicated that precipitation of a 100% aqueous Pt solution rapidly occurred under UV exposition. It suggests that an excess of water promotes a photo-reaction not only at the film surface but also in the bulk of the solution. This mechanism would involve diffusion in the solution of some photo-radicals generated under UV light [11]. It is not excluded that, for a 80% water solution, such a mechanism also occurs in less extent. It would explain that, though no precipitation could be observed even after a long period of UV exposure, this solution yielded larger clusters than a pure ethanolic solution. Let us note that Kim et al. did not report on Pt precipitation when using a pure water solution of chloroplatinic acid [19]. However, their concentration of chloroplatinic acid was more than 50 times smaller than ours. It would suggest an important influence of the chloroplatinic acid concentration, which will be the object of future studies. Fig. 1b and d also show that the platinum coverage progressively increases when increasing the platinization duration and small platinum clusters tend to coalesce at the film surface. This mechanism is particularly marked for a pure ethanolic solution, which yields a more complete coverage of the $TiO_2$ surface by Pt clusters. However, for reasons discussed hereafter, any total coverage of the $TiO_2$ film surface could not be observed even after long photo-platinization durations. Finally, while a post-platinization heat-treatment did not significantly influence the Pt cluster sizes up to a temperature of 400 °C (not illustrated here), Fig. 2b and d show that a heat-treatment at 500 °C promoted an appreciable cluster growth. This feature is essentially observed for the smallest Pt clusters. It suggests that, at 500 °C, the mobility of Pt atoms is sufficient for allowing sintering of vicinal clusters.

In order to investigate the platinization kinetics under UV exposition, we studied the time dependence of the Pt (Mα)/Ti (Kα) intensity ratio deduced from EDX analysis. These variations are illustrated in Fig. 3. For short UV exposures, the EDX accuracy did not allow any reliable differentiation between platinization rates from 0/100 and 80/20 water/ethanol solutions. However, long UV exposures clearly show that the amount of loaded Pt is much important in the case of a water-rich solution. This observation can probably be related to a greater amount of large Pt clusters loaded on the film surface, as evidenced from FEG-SEM images. Though a water rich solution yields a less complete coverage of the $TiO_2$ surface than a pure ethanolic solution, as illustrated Fig. 1b and d, it can yield a much greater volume of loaded platinum that is detected by EDX. Fig. 3 also suggests that, for both studied Pt solutions, the platinization kinetics proceeds through a 3-regime mechanism. Platinization slowly proceeds over the first hour of UV exposure, which can be considered as an ignition period of the platinization process. The kinetics dramatically accelerates over the subsequent hours of UV exposure. It is inferred that, when platinum clusters are loaded in sufficient amount on the film surface, they efficiently act on the separation of photo-generated charge carriers. It yields an increase of the platinization rate owing to a greater amount of photo-electrons that interact with chloroplatinic acid adsorbed at the $TiO_2$ surface. In a third regime, occurring after about 3 h UV exposure, the platinization kinetics is observed to noticeably decelerate. It has been reported that excessive loading of Pt clusters can screen the $TiO_2$ surface from UV light and/or Pt clusters in excess can play a role of recombination centres for photo-generated electrons and holes [3,4,11,19]. In both cases, the photocatalytic activity of the film is expected to fall down leading to a much weaker platinization rate. The plateau observed after 3 h UV exposure explains in turn FEG-SEM images showing that a long photo-platinization procedure does not yield a total Pt coverage of the $TiO_2$ film surface. It should be mentioned that, while the amount of platinum was fairly well controlled in the first and third platinization regimes, no reproducible platinum loading could be achieved in the second regime owing to the aforementioned acceleration of the platinization kinetics. For this reason, in following sections, we only report on the photocatalytic properties of films platinized for 120 min or less.

### 3.2. *Chemical state of Pt clusters*

XPS was used to investigate the chemical state of Pt clusters. Fig. 4 shows XPS spectra in the Pt*4f* region for 0/100 and 80/20 films platinized for 1 h and subsequently heat-treated for 2 h at 110 °C. The former film exhibits a $Pt4f_{7/2}$:$Pt4f_{5/2}$ doublet located at much lower energy than the latter one. Though the amount of loaded Pt was rather weak and did not yield highly resolved spectra, the Pt4f doublet could be deconvoluted into three sets of doublets. For all films studied in the present work, the binding

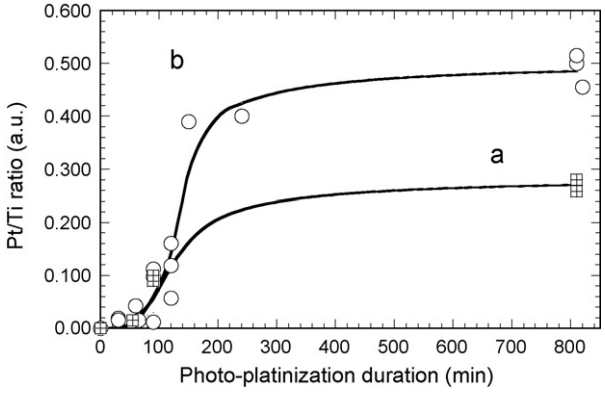


Fig. 3. Platinization duration dependence of the Pt/Ti intensity ratio as determined from EDX analysis for (a) 0/100 and (b) 80/20 films.

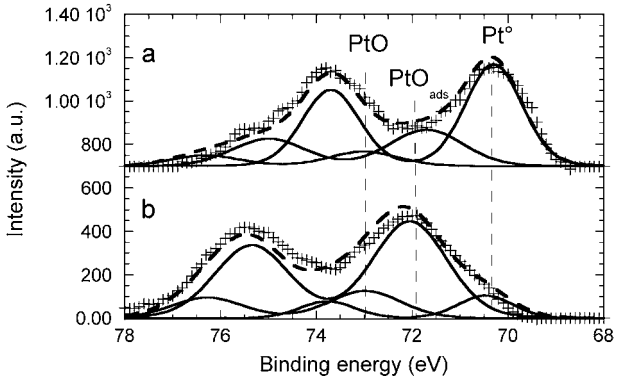


Fig. 4. XPS spectra in the Pt4f region for (a) 0/100 and (b) 80/20 films platinized for 1 h and subsequently heat-treated for 2 h at 110 °C. "+" symbols show the experimental spectra and lines show the deconvoluted spectra.

energies (half-band widths) of the three $Pt4f_{7/2}$ components were determined to be around 70.5 eV (1.4 eV), 71.8 eV (1.8 eV), and 73.1 eV (1.8 eV), within an uncertainty range of ±0.3 eV (±0.1 eV). These values fairly agree with previously published works, which assigned the three components, from low to high energy, to metallic $Pt^0$, Pt with adsorbed oxygen ($PtO_{ads}$), and oxidized $Pt^{2+}$ (PtO) [3,23]. It should be mentioned that the exact assignment of a $Pt4f_{7/2}$ component located at around 72 eV is not totally clear since several authors have also assigned such a component to a $Pt^{2+}$ chemical state [10,16,17,24–26]. In any cases and as mentioned by several authors, the presence of $PtO_{ads}$ and/or PtO species does not mean that the photoreduction of $Pt^{4+}$cations is limited to the +2 valence, but it more probably results from the known tendency of oxygen to rapidly chemisorb on a clean platinum surface during storage under ambient conditions [3,10,23]. In particular, the larger the surface area of Pt clusters, the faster they should be oxidized. Therefore, the presence of chemisorbed or oxidized Pt species essentially arises from the smallest clusters and indicates their high dispersion on the $TiO_2$ surface [3]. In addition, chemisorbed or oxidized Pt species can also result from a combination with $OH^-$ ions [25,26]. Accordingly, spectra of Fig. 4 show that, while the PtO contribution to the Pt4f doublet is rather weak for both 0/100 and 80/20 films (around 10 and 20% of the total Pt4f intensity, respectively), the latter film exhibits a much intense $PtO_{ads}$ component than the former one (around 70% of the total Pt4f intensity compared to 30%). This difference can presumably, at least partially, be attributed to water adsorption occurring on Pt clusters during photo-platinization in aqueous solution. This intense $PtO_{ads}$ component explains in turn why 80/20 films exhibit a Pt4f doublet located at higher energy than 0/100 films.

Fig. 5 shows the intensity of $Pt^0$ and $PtO_{ads}$ components for 80/20 films platinized for 1 h and subsequently heat-treated for 2 h at various temperatures. Since the PtO component did not significantly vary with temperature (10 to 20% of the total Pt4f intensity, which lies in the uncertainty of our deconvolutions), it has not been illustrated in this figure. It is observed that the $Pt^0$ and $PtO_{ads}$ intensities do not evolve when increasing the heat-treatment temperature up to 400 °C, which illustrates the thermal stability of metallic $Pt^0$ and chemisorbed platinum. Further increase to 500 °C yields a noticeable increase (decrease) of the relative amount of $Pt^0$ ($PtO_{ads}$) species. A decrease in the $PtO_{ads}$ amount can first be associated to a thermal desorption of oxygen or water initially chemisorbed at the metal surface. It can also be related to a size increase of Pt clusters, as illustrated in Fig. 2 for films annealed at 500 °C. As the clusters increase in size, *i.e.* their surface area decreases, the contribution of chemisorbed Pt species should logically decrease. In addition, it appears from Fig. 5 that the $PtO_{ads}$ decrease ($Pt^0$ increase) is more pronounced at the film surface (30° take-off angle) than in deeper layers (90° take-off angle), *i.e.* after heat-treatment at 500 °C, the Pt4f doublet appeared shifted toward higher energies when measured with a 90° rather than a 30° take-off angle. In the case of platinized $TiO_2$ films subsequently calcinated at 400 °C, Zhang et al. also mentioned a Pt4f shift toward higher energies, which was all the more pronounced as deeper layers were probed [16,17]. The authors attributed this shift to a strong Pt–$TiO_2$ interaction related to a thermal diffusion of Pt within the $TiO_2$ lattice. It has also been reported that Pt metal can promote a phase transformation from anatase to rutile [27], which would confirm the ability of Pt atoms to enter the $TiO_2$ lattice and induce structural changes. According to conclusions of Zhang et al., Fig. 5 suggests that, in our conditions, a Pt diffusion within the $TiO_2$ film does not take place in much extent up to 400 °C and may appreciably occur at 500 °C. Besides, Pt cluster growth observed after annealing at 500 °C (Fig. 2) confirms the mobility of Pt atoms at this temperature, which might in turn favour diffusion within the $TiO_2$ film. Fig. 6 shows the temperature dependence of the Pt4f integrated intensity normalized to the $Ti2p_{3/2}$ peak (binding energy of 258.7 eV) for films illustrated in Fig. 5. This normalization provides information on the overall surface Pt loading. After heating at 110 °C, the Pt/Ti intensity ratio appears greater when measured with a 30° rather than a 90° take-off angle, which confirms that photo-platinization yields platinum clusters located at the external surface of $TiO_2$ films. Fig. 6 indicates that the surface Pt loading slightly decreases when increasing the temperature up to 400 °C, which is accompanied with a decrease of the $Pt^{30°}/Pt^{90°}$ intensity ratio. After heating at 500 °C, the Pt

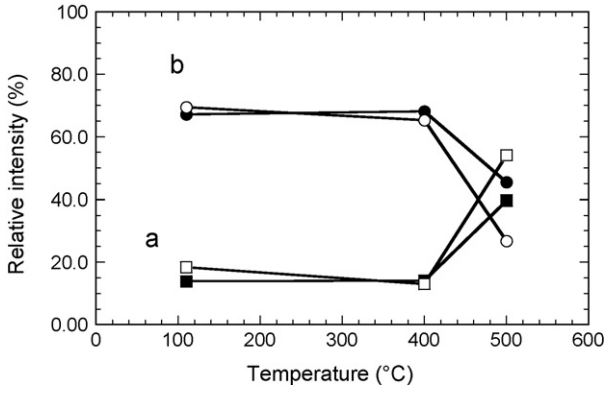


Fig. 5. Intensity of (a) $Pt^0$ and (b) $PtO_{ads}$ XPS components for 80/20 films platinized for 1 h and subsequently heat-treated for 2 h at various temperatures. $Pt^0$ and $PtO_{ads}$ components have been normalized with respect to the total Pt4f doublet intensity. Open and full symbols show data acquired with a take-off angle of 30° and 90°, respectively.

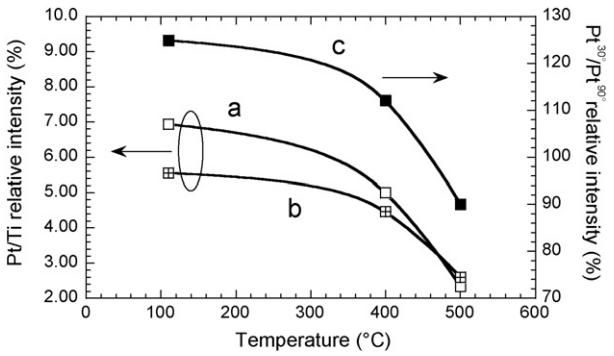


Fig. 6. Temperature dependence of the Pt4f integrated intensity normalized to the $Ti2p_{3/2}$ peak for films illustrated in Fig. 5: (a) 30° take-off angle, (b) 90° take-off angle, and (c) data of (a) normalized to data of (b).

loading decrease is much more pronounced and it is accompanied with an accentuated decrease of the $Pt^{30°}/Pt^{90°}$ intensity ratio. These data, which traduce an impoverishment of surface platinum compared to the amount of platinum in the deeper layers of the platinized films, seem confirming a thermal diffusion of platinum within the $TiO_2$ film. This diffusion would start in small extent at around 400 °C, in agreement with results of Zhang et al., and would take place in much greater extent at 500 °C. However, in the present state, it is difficult to assess whether this diffusion promotes a substitutional or an interstitial $TiO_2$ doping.

### *3.3. Adsorption of photo-platinization by-products*

As mentioned in introduction, an optimal photo-platinization involves the use of a sacrificial oxidizable additive, ethanol in the present work. Thus, ethanol photo-oxidation by-products can adsorb in significant amount at the $TiO_2$ film surface in the course of the platinization process. These adsorbed species can in turn negatively influence the photocatalytic activity of titanium oxide [27]. This is the reason why, in the present work, we particularly focused on the effects of a post-platinization heat-treatment, in order to evaluate to which extent a thermal decomposition of ethanol oxidation by-products could improve the photocatalytic activity of our platinized films. FTIR spectroscopy was used to assess the film contamination by ethanol by-products. For this study, photo-platinization treatments were performed for 14 h in order to maximize the amount of contaminant and allow an accurate detection. Insert of Fig. 7 shows the typical FTIR spectrum of a non-platinized $TiO_2$ film in the low wavenumber spectral region. The spectrum exhibits two strong bands located at 435 and 260 $cm^{-1}$, together with a weak and broad shoulder around 750 $cm^{-1}$, which are assigned to two TO vibration modes of anatase for the formers and a combination of LO modes for the latter [28]. Curve b in Fig. 7 shows the typical spectrum of a 80/20 film photo-platinized for 14 h without post-platinization heat-treatment. In the C–O stretching region, several well-defined bands appear between 1700 and 1000 $cm^{-1}$ together with a strong band at 2070 $cm^{-1}$. It has been

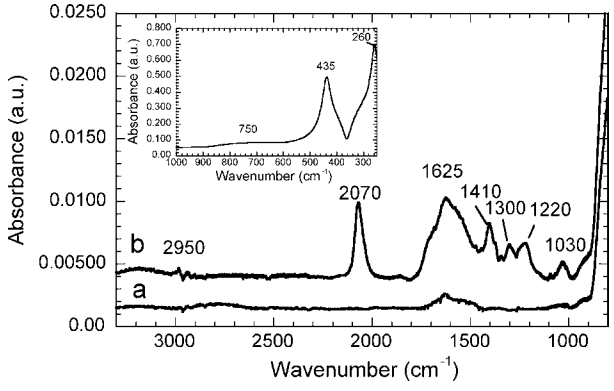


Fig. 7. FTIR spectra of a $TiO_2$ film (a) before and (b) after photo-platinization for 14 h from a 80/20 water/ethanol solution. No post-platinization heat-treatment was performed. Insert shows the typical FTIR spectrum of a non-platinized $TiO_2$ film in the low wavenumber spectral region.

shown that adsorption of ethanol at the surface of metal oxides proceeds through the scission of the ethanol O–H bond and the formation of adsorbed ethoxides [29]. Then, photo-oxidation of ethanol can proceed through numerous decomposition pathways and yield multiple reaction products. For instance, gas chromatography analyses have shown that the oxidation of ethanol at the surface of $TiO_2$ and $Pt/TiO_2$ catalysts yields the formation of gaseous aldehydes (acetaldehyde, formaldehyde) and carboxylic (acetic, formic) acids [7,30,31]. Thus, the spectrum illustrated in Fig. 7b probably corresponds to combinations of multiple bands arising from a wide variety of adsorbed species, which hampers its exhaustive interpretation. Well defined bands located at 1030 and 1300 $cm^{-1}$ may in particular be assigned to C–O stretching modes of ethoxide species [29,32] and carboxylic acids [33], respectively. These species can in turn partly contribute to IR bands observed between 1700 and 1300 $cm^{-1}$. The presence of ethoxides at the surface of our films would indicate that photo-platinization did not yield a complete oxidation of adsorbed ethanol. Curve b in Fig. 7 also depicts very weak bands at around 2950 $cm^{-1}$, which might correspond to C–H stretching modes of non-oxidized ethoxide species or organic oxidation by-products. However, these latter bands were too small for allowing reliable analysis. It is worthwhile mentioning that all the bands illustrated in curve b of Fig. 7 were not detected for non-platinized films (curve a in Fig. 7), except a weak band around 1625 $cm^{-1}$, which is assigned to the bending mode of molecular water arising from atmospheric moisture adsorbed at the $TiO_2$ film surface. As discussed hereafter, most of the bands observed between 1700 and 1000 $cm^{-1}$ as well as the band at 2070 $cm^{-1}$ are attributed to ethanol by-products. Chloroplatinic photo-decomposition products might also contribute to these bands, but since chloroplatinic acid/ethanol molar ratios in our solutions were fixed at extremely small values of around $10^{-5}$ to $10^{-4}$, it is inferred that only ethanol by-products can be detected in FTIR spectra. Additional bands of ethoxide species and photo-oxidation by-products could not be observed below 1000 $cm^{-1}$ since they were probably overlapped by more intense anatase LO and TO modes. In this section and in the next one, we focus therefore on bands located between 1700 and 1000 $cm^{-1}$. The band located at 2070 $cm^{-1}$ is discussed in Section 3.5.

Fully reproducible IR spectra could not be obtained directly after photo-platinization, which indicates that some unstable species were adsorbed at the film surface and could easily desorb at room temperature. Thus, curve b in Fig. 7 is only provided as a typical example. Reproducible spectra were obtained after heat-treatment at 110 °C or more, which are illustrated in Fig. 8A–C, for 0/100, 50/50, and 80/20 films, respectively. Bands observed between 1300 and 1000 $cm^{-1}$ in curve b of Fig. 7 could no longer be observed after heating at 110 °C (not illustrated here). This disappearance presumably indicates a total decomposition of remaining ethoxide species and desorption of a first generation of unstable photo-oxidation by-products. In the 1700–1300 $cm^{-1}$ range, spectra obtained after heat-treatment at 110 °C (Fig. 8A(a)–C(a)) consist of a broad band with two maxima at around 1625 and 1540 $cm^{-1}$, a sharper band at around 1410 $cm^{-1}$, and a weaker one at around 1345 $cm^{-1}$. As shown in curve b of Fig. 7, these bands were already detected before

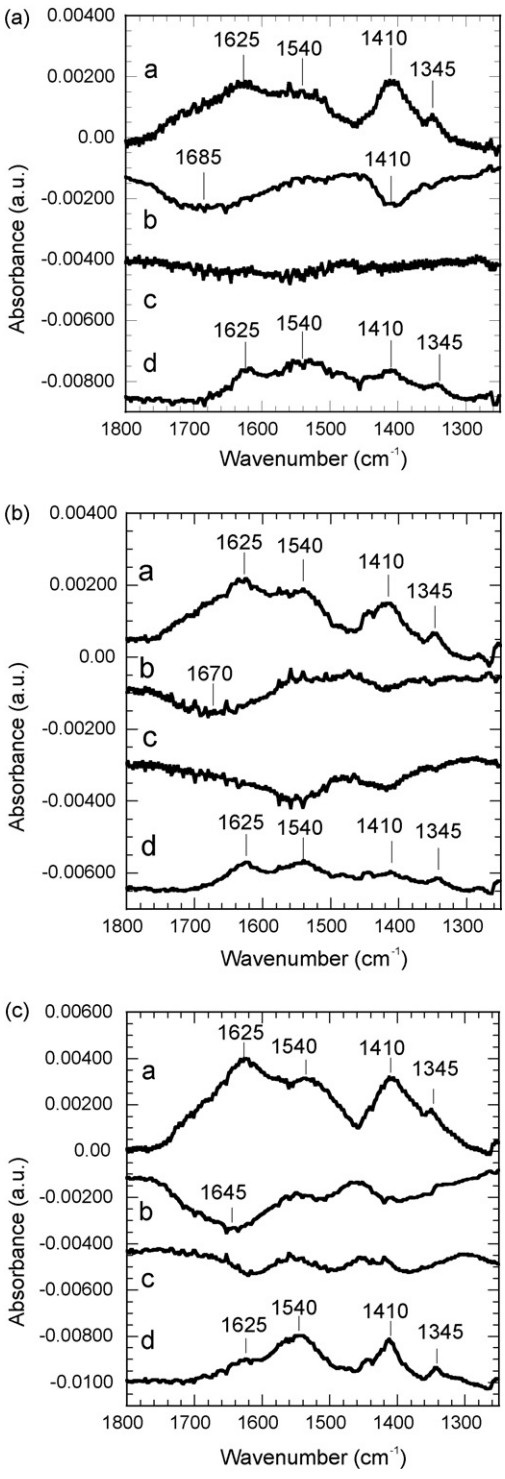


Fig. 8. FTIR spectra of (A) 0/100, (B) 50/50, and (C) 80/20 $TiO_2$ films photo-platinized for 14 h and subsequently heat-treated for 2 h at various temperatures: (a) spectra after heat-treatment at 110 °C, (b) differential spectra 250–110 °C, (c) differential spectra 500–250 °C, and (d) spectra after heat-treatment at 500 °C. Negative bands in differential spectra indicate the disappearance of chemical species in the investigated thermal ranges. All spectra are presented in comparable absorbance scales.

heat-treatment. It is worthwhile noting that these spectra fairly agree in their band positions and intensities with those reported by other authors for ethanol oxidation by-products adsorbed at the surface of platinized $CeO_2$ catalysts [29,34]. Thus, according to these authors, we can tentatively assign bands located at 1540, 1410, and 1345 $cm^{-1}$ to C–O stretching modes of adsorbed carboxylates and/or carbonates, which would derive from the oxidation of adsorbed ethoxide species and photo-oxidation by-products such as aldehyde species and carboxylic acids. Bands at 1540 and 1345 $cm^{-1}$ would correspond to a carboxylate and/or bidentate carbonate species. Accordingly, several authors have mentioned similar bands for carboxylates and bidentate carbonates adsorbed at the surface of non-platinized $TiO_2$ [33,35]. The band at 1410 $cm^{-1}$ has been assigned either to a carboxylate or to a symmetric carbonate species [29,34]. Finally, a broadening of the 1540 $cm^{-1}$ band towards higher wavenumbers, which produces a second maximum around 1625 $cm^{-1}$, can arise from several features. Firstly, it can be due to molecular water adsorbed at the film surface after the heat-treatment at 110 °C. Remaining carboxylic acids might also eventually contribute to this maximum [33]. Besides, the high wavenumber broadening of this band might be attributed to a combination of several components between 1700 and 1600 $cm^{-1}$, which would arise from remaining aldehyde species [34]. These species are produced via an oxidative dehydrogenation of ethanol. They were observed as intermediary adsorbed by-products in the thermal decomposition of ethanol to carboxylates and carbonates at the surface of platinized $CeO_2$ [34]. As shown in Fig. 8A(a)–C(a), heat-treatment at 110 °C yielded rather similar spectra for the three studied solutions. The only salient feature is the greater intensity of bands observed in the case of a 80/20 water/ethanol solution (Fig. 8C(a)), which would indicate that this solution favours a more efficient ethanol photo-oxidation yielding a greater amount of oxidation by-products.

### *3.4. Thermal decomposition of photo-platinization by-products*

Fig. 8A(d)–C(d) show IR spectra acquired after heating Pt–$TiO_2$ films at 500 °C. Bands observed in Fig. 8A(a)–C(a) have decreased in intensity, but are still present, which indicates the relative thermal stability of some ethanol photo-oxidation by-products. A small band at 1625 $cm^{-1}$ can be attributed to water adsorbed at the film surface, as previously illustrated in Fig. 7a for a non-platinized film heat-treated at 500 °C. Other bands at 1540, 1410, and 1345 $cm^{-1}$ probably correspond to carbonates, which are the most likely species able to persist after a heat-treatment at 500 °C. After such a treatment, these three bands remained more intense in the case of a 80/20 film (Fig. 8C(d)) than for 0/100 (Fig. 8A(d)) and 50/50 (Fig. 8B(d)) films. It does not mean that thermal decomposition of photo-oxidation by-products is less efficient for the former film, but more presumably indicates that photo-oxidation in a water-rich solution yields more stable oxidation by-products, which confirms that such a solution favours a more efficient ethanol photo-oxidation. This conclusion is confirmed by differential spectra illustrated in Fig. 8A(b,c)–C(b,c). These spectra indi-

cate that decomposition and/or desorption of a second generation of oxidation by-products mainly occurs in the 110–250 °C thermal range (Fig. 8A(b)–C(b)). Differences observed between 250 and 500 °C (Fig. 8A(c)–C(c)) were too weak to permit reliable interpretations. Fig. 8A(b)–C(b) show that decomposition and/or desorption occurring between 110 and 250 °C proceed through different pathways, which depend on the water/ethanol composition of the Pt solution. For a 0/100 film, the differential spectrum of Fig. 8A(b) consists of a negative broad band located at around 1685 $cm^{-1}$ together with a negative band at 1410 $cm^{-1}$. For 50/50 (Fig. 8B(b)) and 80/20 (Fig. 8C(b)) films, differential spectra essentially consist of a negative band located at around 1670 and 1645 $cm^{-1}$, respectively. It can first be argued that decomposition of rather unstable aldehyde species or carboxylic acids contributes to the 1685–1645 $cm^{-1}$ negative bands. Besides, a shift of this negative broad band from 1685 to 1645 $cm^{-1}$ with increasing the amount of water in the Pt solution might indicate that such unstable species, which contribute to a high wavenumber broadening of the 1625–1540 $cm^{-1}$ dual band, are initially present in lesser amount in the case of a water rich solution. In other words, photo-oxidation in ethanol rich solution would promote a greater extent of unstable intermediary species, which would require a post-platinization heat-treatment at sufficiently high temperature to be decomposed in more stable carboxylate or carbonate species. Conversely, a water rich solution would promote a more complete photo-oxidation of ethanol into stable species that yield more intense carboxylate and/or carbonate IR bands, as observed in the spectrum of Fig. 8C(a). This conclusion is supported by works of Sakata et al. who studied gaseous oxidation by-products formed during the $TiO_2$-assisted photocatalytic decomposition of ethanol [30]. These authors indicated that, in the absence of water, the main decomposition pathway yielded the formation of gaseous acetaldehyde, while the presence of water, by inducing the photo-generation of strongly oxidant $OH^0$ radicals, could promote a complete oxidative decomposition of ethanol into $CO_2$. These data clearly show that photo-oxidation of ethanol can proceed in greater extent in presence of a water excess.

### *3.5. Adsorption and desorption of CO*

Previous observations can be completed by an analysis of Fig. 9, which shows intensity variations of the 2070 $cm^{-1}$ band versus post-platinization temperature for the three studied Pt solutions. Owing to its position, this band can unambiguously be attributed to carbon monoxide CO species linearly coordinated to metallic Pt sites [3,26,29]. This observation is in agreement with the known tendency of CO to strongly adsorb on Pt metal, which can in turn seriously alter the photo-activity of Pt–$TiO_2$ catalysts [26]. The absence of additional bands at around 2000 $cm^{-1}$ and between 2200 and 2100 $cm^{-1}$ (see Fig. 7b) indicates that eventual CO species, which would weakly bond on $Pt^{2+}$ or $TiO_2$ sites, have desorbed immediately after photo-platinization [3,26]. A more or less intense CO band was detected after photo-platinization in the three studied Pt solutions. As explained before, fully reproducible IR spectra could not be obtained directly after photo-platinization, which

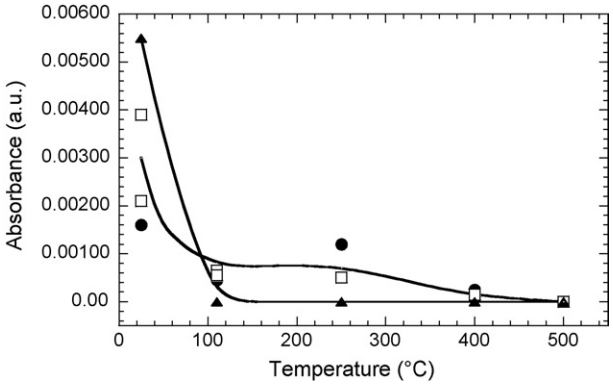


Fig. 9. Intensity variations of the 2070 $cm^{-1}$ CO IR band versus post-platinization temperature for 0/100 (□), 50/50 (●), and 80/20 (▲) films.

hampered a reliable analysis of the CO band intensity before heat-treatment. For the three solutions, Fig. 9 shows that the CO band strongly decreases in intensity after heating at 110 °C. It was difficult to quantitatively analyze intensity variations of this band in relation to the post-platinization temperature owing to its weak intensity. Nevertheless, a clear distinction can be made between the 80/20 water/ethanol solution and both other ones. For the former solution, any CO band could no longer be observed after heating at 110 °C. For both other solutions, intensity of this band gradually decreased with raising temperature and the CO band completely disappeared only after heat-treatment in the 400–500 °C thermal range. This observation seems to disagree with previous works showing that CO pre-adsorbed on a Pt surface usually desorbs at relatively low temperature and desorption is almost complete at around 200 °C [26]. Thus, in the case of 0/100 and 50/50 films, data of Fig. 9 suggest that new CO species are formed and remain adsorbed at the Pt surface during heat-treatment in the 110–400 °C thermal range, which would not be the case for a 80/20 film.

Previous papers dealing with the thermal oxidation of ethanol at the surface of $TiO_2$ and Pt–$TiO_2$ catalysts did not report on the formation of CO as an oxidation product but only mentioned a gaseous $CO_2$ production [7,31]. However, the authors focused on gaseous oxidation products analysed by gas chromatography and they did not provide IR spectra of the catalyst support. Conversely, FTIR spectroscopy was used to study the thermal oxidation of ethanol at the surface of platinized $CeO_2$. These studies evidenced the persistence of a CO band up to 300–400 °C, showing that CO could remain adsorbed on platinum at a relatively high temperature [29,34]. These works suggest that CO can, (i) be produced from the direct decomposition of ethoxide species adsorbed at the catalyst surface, presumably through a C–C bond dissociation, and (ii) appear as an adsorbed by-product in the oxidation of ethoxide to carboxylate or carbonate species. In particular, IR spectroscopy studies have shown that thermal oxidation of actetaldehyde at the surface of metallized $CeO_2$ occurs through the formation of adsorbed CO [36]. According to these data, we infer that, as far as ethanol has not been fully decomposed into stable carboxylate or carbonate species, a thermal treatment in oxidizing conditions can produce CO adsorbed on Pt sites. Fig. 8A–C

suggest that 0/100 and 50/50 water/ethanol solutions promote a less efficient ethanol photo-oxidation than a 80/20 solution. Photo-oxidation can yield a greater extent of unstable aldehyde species or carboxylic acids in the case of both former solutions, and oxidation of these species to more stable ones requires a post-platinization heat-treatment at relatively high temperature. This treatment might conjointly promote desorption of initially adsorbed CO and adsorption of newly formed CO arising from a complementary oxidation reaction. It would explain the detection of a CO band after heat-treatment at temperatures up to around 400 °C.

Since a 80/20 water/ethanol Pt solution promotes a more complete photo-oxidation of ethanol leading to more stable oxidation by-products, it can be supposed that these stable species do not undergo any complementary oxidation during heat-treatments at temperatures greater than 110 °C. It would reduce further formation of adsorbed CO at these temperatures. However, this explanation cannot fully account for the total lack of detection of a CO band after heat-treatment at 110 °C or more. Indeed, spectra of Fig. 8C indicate that, even for a 80/20 film, some unstable species are still present after heat-treatment at 110 °C and essentially disappear after heating at 250 °C. It suggests that CO should be detected after heat-treatment in the 110–250 °C thermal range in relation to the complementary oxidation of these species. Since it is not the case, another mechanism has to be taken into account, which might be related to the fact that photo-platinization in presence of a water excess promotes a much more important quantity of $PtO_{ads}$ species than photo-platinization in ethanol rich solution, as shown by XPS. It has been reported that oxygen or water chemisorbed onto a Pt surface can readily react with adsorbed CO to promote its oxidation in gaseous $CO_2$ and/or can induce modifications in the electronic properties of Pt, thus affecting the adsorptive bond strength of CO species [26]. In both cases, chemisorbed oxygen or water induced by a water rich Pt solution can thus prevent adsorption of CO that would eventually be produced during a heat-treatement at 110 °C or more. It would not be the case for Pt solutions with a too small water fraction, owing to the formation of a much smaller quantity of $PtO_{ads}$ species. Finally, it is worthwhile mentioning that a premature CO disappearance, *i.e.* an optimal photo-oxidation of ethanol, requires a strong water excess, since data of Fig. 9 show that a 50/50 water/ethanol does not yield results significantly different from a 0/100 solution.

### *3.6. Characterization of the photocatalytic activity*

Fig. 10 shows typical variations of the decomposed OG molar fraction versus UV exposition duration for different platinized films. Insert of Fig. 10 shows similar variations for several non-platinized films elaborated in identical conditions. Variations illustrated in the insert indicate that the term $\ln(C_0/C)$ linearly increases with the UV exposition time over the three first hours of exposition. Thus, for non-platinized films, the photocatalytic reaction follows an apparent first-order [37]. Previous works have shown that, in the presence of a $TiO_2$ photocatalyst, OG not only undergoes a photo-decolorization but is also efficiently photocatalytically decomposed [38]. In order to assess

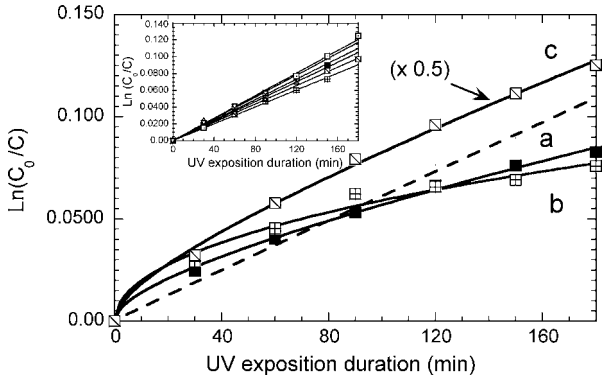


Fig. 10. Molar fraction of decomposed OG versus UV exposition duration for (a) 0/100, (b) 50/50, and (c) 80/20 films photo-platinized for 1 h and subsequently heat-treated at 110 °C. In curve (c), the molar fraction of decomposed OG has been normalized by a factor 0.5 to allow a better clarity of this figure. Insert illustrates the same variations for different non-platinized films elaborated in identical conditions. In the main figure, the dotted line corresponds to an averaged variation deduced from data of insert.

the apparent rate constant ($k$) of the photocatalytic reaction, we considered the slopes derived from the $\ln(C_0/C) = f(t_{UV})$ variations. An average $k$ value of $0.035 \pm 0.005\ h^{-1}$ was deduced for non-platinized films illustrated in the insert. The $\pm 0.005\ h^{-1}$ dispersion can partly be attributed to the measurement error. It probably also indicates a certain non-reproducibility in the film physico-structural properties that govern the photocatalytic reaction, as discussed in our previous articles [21,22]. In this section, $0.035\ h^{-1}$ will be taken as a reference $k$ value for non-platinized films and $\pm 0.005\ h^{-1}$ will be considered as the experimental error. Contrary to non-platinized films, data of Fig. 10 indicate that the photocatalytic reaction induced by platinized films does not follow a first-order. The molar fraction of decomposed OG increases rapidly over the first stages of UV exposition. Then, the photocatalytic reaction is observed to decelerate and the $\ln(C_0/C)$ term starts to linearly increase with further increase of the UV exposition time, *i.e.* the reaction starts to follow an apparent first-order. This bi-regime behaviour suggests that the reaction first proceeds through a more or less fast transitory regime before that a slower steady state regime be established. As will be discussed hereafter, these features strongly depend on the platinization conditions and post-platinization heat-treatments. In this study, $\ln(C_0/C) = f(t_{UV})$ variations in the transitory regime have been arbitrarily fitted with a two-order polynomial function by taking into account values measured over the first 90 min of UV exposure. The steady state regime has been fitted with a linear function using values measured over the subsequent 90 min of UV exposure. These fits were used to allow a quantitative comparison of the rate constants in both regimes, *i.e.* a $k_1$ value deduced from the slope at the origin of the polynomial function and a $k_2$ value deduced from the slope of the linear function were used to assess the initial rate constant and the rate constant in the second regime, respectively. In following parts of this article, we study how $k_1$ and $k_2$ values can be optimized with respect to experimental conditions, keeping in mind that an optimal platinization should yield a high $k_1$ value, which indicates an optimal activity in the first photo-

catalysis regime, together with a $k_2$ value as close as possible to the $k_1$ value, which indicates minimization of the deceleration in the second photocatalysis regime. As shown in Fig. 10, any significant difference could not be observed in the photocatalysis kinetics of 0/100 and 50/50 films. For this reason, the latter films will not be further considered in this section.

Fig. 11a and b illustrate the photo-platinization duration dependence of $k_1$ and $k_2$, respectively, for 0/100 and 80/20 films heat-treated at 110 °C. For the former films, the $k_1$ value first increases with the platinization duration, reaching a maximal value after about 20–30 min platinization, after what $k_1$ continuously decreases with further increase of the platinization duration. The $k_2$ value measured for these films is observed to continuously decrease with the platinization duration. As a consequence of this very slow second regime, after an UV exposition exceeding 2 h, the photocatalytic activity of 0/100 films platinized for 20 min or more was observed to drop below that measured for non-platinized films (see Fig. 10a), which indicated that platinum clusters globally impinged the photocatalytic activity of 0/100 films. Fig. 11a shows that the $k_1$ value measured for 80/20 films increases with increasing the platinization duration, reaching a maximal value after about 30 min platinization. This value does not appreciably vary when further increasing the platinization duration up to 2 h. This maximal $k_1$ value is about four times greater than the $k$ value measured for non-platinized films and it is significantly greater than the maximal $k_1$ value measured for 0/100 films. Besides, the $k_2$ value measured for 80/20 films is observed to continuously increase when increasing the platinization duration up to 90 min. Further increase of the platinization duration did not yield any improvement of the $k_2$ value and both $k_1$ and $k_2$ were observed to fall down for platinizations longer than 2 h (not illustrated here), similarly to what was observed for 0/100 films platinized for more than 20–30 min. Though the maximal $k_2$ value reached for 80/20 films remains weaker than the corresponding $k_1$ value, which indicates that even these films undergo a bi-regime photocatalytic reaction, this maximal $k_2$ value is 2.7 times greater than that measured for non-platinized films. Consequently, photocatalytic activities of 80/20 films platinized for 2 h or less appeared systematically much higher than those of non-platinized films, even after a long term UV exposition (see Fig. 10c), showing in that case the beneficial effect of platinum clusters. From these data, it appears that improved photo-activities of platinized films rely on, (i) a platinization in water rich Pt solution, and (ii) an optimal platinum loading that is reached, in our experimental conditions, after a 90–120 min platinization.

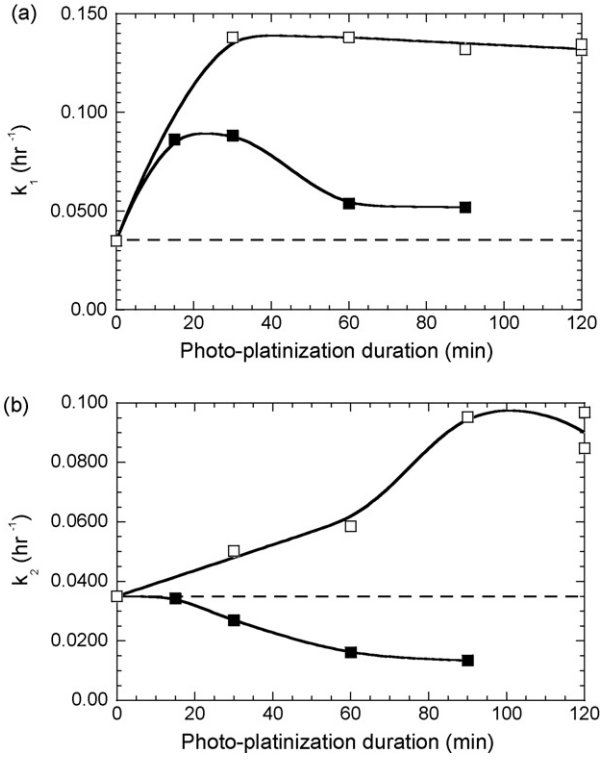


Fig. 11. Influence of the platinization duration on the (a) $k_1$ and (b) $k_2$ values for 0/100 (■) and 80/20 (□) films heat-treated at 110 °C. The dotted line indicates the averaged $k$ value deduced from insert of Fig. 10 for non-platinized $TiO_2$ films.

Fig. 12 illustrates $k_1$ and $k_2$ variations versus post-platinization heat-treatment temperature for 0/100 films platinized for 60 min and 80/20 films platinized for 120 min. In the case of 0/100 films, increasing the post-platinization temperature up to 400 °C promotes a slight improvement of the $k_1$ value, but this value remains much weaker than best values depicted in Fig. 11a for 80/20 films. Further increase of the temperature up to 500 °C yields a slight decrease of the $k_1$ value. At any temperatures, the corresponding $k_2$ value remains extremely weak and well below the $k$ value measured for non-platinized films. In the case of 80/20 films, increasing the post-platinization temperature up to 400 °C does not yield any significant variation of the $k_1$ value, which remains as high as that measured after heat-treatment at 110 °C. The $k_2$ value slightly increases when increasing the temperature up to 250 °C, reaching a maximal value that is about three times greater than the $k$ value measured for non-platinized films. Further increase of the temperature up to 400 °C does not yield any improvement. 80/20 films heated at 500 °C exhibit a dramatic drop of their $k_1$ and $k_2$ values, the former turning close to that evidenced for 0/100 films heated at 500 °C and the latter turning weaker than the

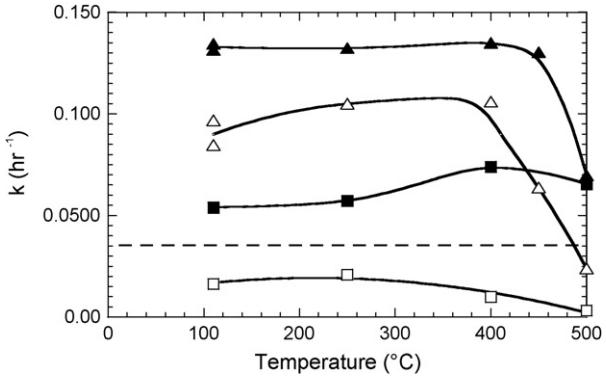


Fig. 12. Influence of the post-platinization heat-treatment temperature on the $k_1$ (full symbols) and $k_2$ values (open symbols) for 0/100 films platinized for 60 min (■, □) and 80/20 films platinized for 120 min (▲, △). The dotted line indicates the averaged $k$ value deduced from insert of Fig. 10 for non-platinized $TiO_2$ films.

$k$ value measured for non-platinized films. These data indicate that, for both studied solutions, there exists an optimal post-platinization temperature comprise between 250 and 400 °C. They also confirm that, whatever be the post-platinization temperature, platinization in the presence of a sufficient water excess yields best photocatalytic performances.

### *3.7. The photocatalytic activity of platinized $TiO_2$ films: discussion*

#### *3.7.1. Bi-regime photocatalysis kinetics*

Our characterizations indicate that the photocatalytic reaction decelerates over a long term UV exposition and this deceleration is dramatically marked when $TiO_2$ films are platinized from a water poor Pt solution. Such behaviour was not observed in the case of non-platinized $TiO_2$ films. Though the beneficial effects of Pt clusters loaded at the surface of a $TiO_2$ photocatalyst are generally well recognized, some authors have also reported on a long term deceleration of photo-reactions induced by Pt–$TiO_2$ photocatalysts [9,39]. It is generally well admitted that optimal photocatalytic activities rely on an efficient photo-electron evacuation from the photocatalyst, which essentially involves a transfer to molecular oxygen present at the photocatalyst surface [9,11,27,39]. Oxygen acts as primary electron acceptor and readily undergoes a cathodic reduction. This transfer to oxygen first reduces the recombination probability of photo-generated holes with photo-electrons. Alternatively, the reduction of oxygen by photo-electrons can induce a multi-step chain reaction producing various kinds of oxidative radicals, which reinforces the anodic oxidative photo-decomposition induced by photo-holes at the photocatalyst surface [11]. The role of oxygen becomes particularly crucial in de-aerated liquid systems, *i.e.* in the absence of air or oxygen bubbling, where the amount of dissolved oxygen is very limited. In that case, the photo-electron transfer to oxygen becomes the rate-controlling step of the photo-induced reactions. As mentioned in introduction, owing to the formation of a Schottky barrier at the metal-semiconductor interface, electrons photo-generated within a platinized $TiO_2$ photocatalyst are readily transferred to and trapped in Pt particles, which promotes an efficient $e^-/p^+$ separation and initially enhances the photocatalytic reaction. However, in a de-aerated liquid system like the one used in this study, the rate of photo-electron transfer from platinum is reduced owing to the limited amount of oxygen dissolved in the liquid. Thus, electrons can accumulate in Pt clusters that progressively become negatively charged. On the one hand, it causes a progressive reduction of the Schottky barrier, which decreases the $e^-/p^+$ separation efficiency. On the other hand, once negatively charged, Pt particles can attract photo-holes that readily recombine with trapped electrons, *i.e.* Pt particles start acting as $e^-/p^+$ recombination centres [11]. Combination of both effects yields a noticeable reduction of the photocatalytic activity, which becomes governed by a competitive process between the separation and recombination mechanisms induced by more or less negatively charged Pt clusters. Such competitive process can presumably account for the bi-regime photocatalytic activity of our Pt–$TiO_2$ films, as illustrated in Figs. 10–12. In a first transitory regime, we have determined a rather high initial rate constant $k_1$, whose variations would essentially traduce the maximal $e^-/p^+$ separation efficiency promoted by neutral platinum clusters in the early stages of the photo-reaction. In a second regime, we have observed an apparent first-order photocatalytic reaction with a weaker rate constant $k_2$ that would essentially traduce a steady state equilibrium between, (i) the flux of charge carriers reaching the film surface, which relies on the photo-generation yield and recombination rate of $e^-/p^+$ during their travel toward the surface, and (ii) the recombination rate induced by more or less negatively charged platinum clusters, which relies on the transfer efficiency of photo-electron toward dissolved oxygen. As discussed below, additional features can also account for the $k_1$ and $k_2$ variations. In the case of non-platinized $TiO_2$ films, the flux of charge carriers reaching the surface should be noticeably weaker than for platinized films owing to a much greater recombination induced by the absence of any Schottky barrier. This conclusion is supported by the rather weak activity of non-platinized films (insert of Fig. 10). Then, it can be supposed that the flux of photo-electrons is weak enough to allow their total transfer to dissolved oxygen, which would explain that any bi-regime behaviour could not be observed for non-platinized films.

#### *3.7.2. Influence of the water/ethanol composition*

For both studied water/ethanol Pt solutions, Fig. 11a shows that the $k_1$ value initially increases with the photo-platinization duration, *i.e.* the amount of loaded platinum, which depicts the beneficial effect of platinum clusters on the $e^-/p^+$ separation. This beneficial effect is less marked in the case of films platinized from a pure ethanolic solution and, for these films, further increase of the platinization duration rapidly yields a $k_1$ decrease. As explained in introduction, such a decrease can first depict that there exists an optimum Pt loading threshold above which platinum clusters detrimentally act on the photocatalytic reaction, (i) by limiting the amount of UV light absorbed by the photocatalyst and the related $e^-/p^+$ generation (shading effect), and (ii) by reducing the amount of Pt-free $TiO_2$ regions where photo-generated holes can induce an anodic oxidation reaction (shielding effect). For films platinized in presence of a water excess, Fig. 11a shows that the maximal $k_1$ value is much higher than for films platinized from a pure ethanolic solution and it is less critically influenced by the platinization duration. It is first inferred that, though the Pt loading rate is greater in the case of a water rich solution (Fig. 3), such solution yields a less complete coverage of the $TiO_2$ surface than a pure ethanolic one (Fig. 1b and d), which can reduce aforementioned shading and shielding effects. As suggested by Figs. 1 and 2, effects of platinum particle sizes might also partially influence differences in the photocatalytic activities of films platinized in presence or absence of water. Furthermore, it has been shown in previous sections that the water/ethanol composition acts on the nature of species adsorbed at the surface of Pt clusters, which can modify electronic properties of these latter and the related Schottky barrier, thus influencing the $e^-/p^+$ separation. The beneficial influence of a water rich Pt solution on the photo-activity of platinized films appears again more marked when considering the $k_2$ variations illustrated in Fig. 11b. While, in the case of films

platinized from a pure ethanolic Pt solution, the $k_2$ value continuously decreases when increasing the platinization duration, films platinized from a water rich solution exhibit a reverse trend, as far as the platinization duration does not exceed 90 min. For these latter films, the $k_2$ decrease observed for longer platinization durations can presumably be attributed to shading and shielding effects. However, these effects cannot fully explain differences observed between 0/100 and 80/20 films for short platinization durations. We believe that adsorbed species depicted by FTIR spectroscopy can partly account for such differences. On the one hand, it seems that various adsorbed carbonated species detected by FTIR spectroscopy in the 1700–1000 $cm^{-1}$ spectral range are of secondary effect on the photocatalytic activity, since films platinized from a water rich solution exhibit the best activity despite a greater amount of adsorbed carbonates species. The secondary effect of such species will be assessed hereafter. On the other hand, Fig. 9 shows that CO is present at the surface of Pt clusters loaded from ethanol rich solutions, even after a heat-treatment above 250 °C, while any CO could not be detected for 80/20 films heat-treated at 110 °C or more. It is known that CO adsorbed at the surface of platinum particles can seriously alter the photo-activity of Pt–$TiO_2$ catalysts [26]. In particular, CO adsorbed at the platinum surface can hamper the photo-electron transfer to dissolved oxygen, which reduces the photocatalytic activity. This feature can explain that the $k_2$ value of 0/100 films continuously decreases when increasing the platinization duration, as illustrated in Fig. 11b. Indeed, as far as these films are not heat-treated at sufficiently high temperature, adsorbed CO should accumulate at the film surface when photo-platinization proceeds, owing to the progress of the related ethanol photo-oxidation. Then a greater amount of adsorbed CO can decrease efficiency of the photo-electron transfer to oxygen during the OG photo-decomposition, which yields an enhanced $e^-/p^+$ recombination induced by more negatively charged Pt clusters. Conversely, since no CO is adsorbed on 80/20 films heat-treated at 110 °C or more, increasing the platinization duration in a reasonable range of time should only promote the expected beneficial effects of a Pt loading, *i.e.* an enhanced $e^-/p^+$ separation yielding an improved photo-activity. This feature can explain that, (i) 80/20 films exhibit the highest $k_1$ and $k_2$ values, and (ii) the $k_2$ value measured for these films increases with increasing the photo-platinization duration up to 90 min. The role of adsorbed CO on the photocatalytic activity seems also to be supported by the correlation between photocatalytic and FTIR data for 0/100 and 50/50 films. Indeed, similarly poor photocatalytic activities were evidenced for these films (see Fig. 10), which were also comparatively affected by CO adsorption, as shown in Fig. 9.

*3.7.3. Influence of the post-platinization temperature*

Fig. 12 shows that the $k_1$ value of 0/100 films slightly increases with increasing the post-platinization temperature up to 400 °C. This feature can provide a new evidence of the CO influence, since Fig. 9 indicates that heating at 400 °C promotes a noticeable decrease in the amount of CO adsorbed on these films. However, two observations suggest that CO contamination does not totally explain differences in the photo-activity of 0/100 and 80/20 films. Despite a noticeable decrease in the CO amount, the improved $k_1$ value measured for 0/100 films after heating at 400 °C never reaches optimal values measured for 80/20 films. Furthermore, heating 0/100 films at 400 °C does not improve their $k_2$ value, contrary to what would be expected from a decrease in the CO amount. XPS data can provide complementary information to explain differences in the photo-activity of platinized films. These data show that, (i) the Pt4f doublet exhibits a more intense $PtO_{ads}$ component in the case of 80/20 films (Fig. 4), and (ii) intensity of this component remains constant when increasing the heat-treatment temperature up to 400 °C (Fig. 5). As explained before, this intense $PtO_{ads}$ component can at least partially be attributed to Pt–OH groups arising from water adsorption during photo-platinization in aqueous solution. It is known that photo-decomposition in aqueous solution relies on a purely oxidative reaction mediated by $OH^0$ radicals, which originate from the oxidation of $OH^-$ surface groups by photo-generated holes [37]. It has been shown that $OH^0$ radicals efficiently act in the oxidative photo-decomposition of OG [38]. During the photocatalytic reaction, Pt–OH groups present at the platinized film surface can be oxidized by holes photo-generated in vicinal Pt-free $TiO_2$ regions. It would produce a greater amount of oxidative $OH^0$ radicals able to decompose OG, which would improve the photocatalytic activity of 80/20 films, yielding enhanced $k_1$ and $k_2$ values. When heated in the 250–400 °C thermal range, films platinized from a water rich solution exhibit a higher $k_2$ value than similar films heat-treated at 110 °C. On the one hand, increasing the post-platinization temperature for such films does not influence the adsorption of CO (Fig. 9) and water (Fig. 5) on Pt clusters. On the other hand, Fig. 8C indicates that the amount of carbonated species gradually decreases when increasing the temperature. Thus, though these species are thought to be of secondary effect on the photocatalytic activity, it is not excluded that reducing their amount can induced a slight photo-activity enhancement, as far as main contaminant species (CO) are fully eliminated. For instance, the presence of adsorbed carbonate species might reduce the amount of surface sites available for OG adsorption, thus reducing the OG photo-decomposition rate. Finally, Fig. 12 shows that all films exhibit a partial loss of photo-activity after a heat-treatment at 500 °C, this trend being particularly marked in the case of 80/20 films. For these films, XPS studies have shown that the $PtO_{ads}$ component of the Pt4f doublet noticeably decreases in intensity after heating at 500 °C, which might traduce a desorption of water adsorbed at the Pt surface and a reduced amount of Pt–OH groups. It would produce a decrease in the amount of photo-induced $OH^0$ radicals yielding a weaker photocatalytic activity. FEG-SEM images also indicate that a heat-treatment at 500 °C promotes modifications in the size and distribution of platinum clusters (Fig. 2). As indicated in introduction, these parameters can noticeably influence the photocatalytic activity of platinized $TiO_2$ photocatalysts. Finally, XPS data suggest that a sufficiently high temperature post-platinization heat-treatment promotes a thermal diffusion of platinum within the films yielding a substitutional or interstitial $TiO_2$ doping. $TiO_2$ doping by metal ions has often been reported to cause a strong decrease in the photocatalytic activity

by promoting an enhanced $e^-/p^+$ recombination (see numerous examples in [11]). Thus, it cannot be excluded that the photocatalytic activity of our films be detrimentally affected by platinum doping effects. For reasons discussed above, the $k_2$ value of 80/20 films increases when increasing the post-platinization temperature up to 250 °C, but it is not improved by further temperature increase up to 400 °C. Since XPS data suggest that platinum diffusion starts in small extent at around 400 °C, the beneficial influence of the heat-treatment might be balanced by some doping effects promoted by the onset of platinum diffusion. In addition, further increase of the temperature up to 500 °C yields a strong decrease of the photo-activity, which might express that, at this temperature, detrimental effects of a platinum doping become preponderant. Accordingly, XPS suggests that Pt diffusion occurs in great extent at 500 °C. However, as mentioned in recent articles, platinum-support interactions can probably have more complex influences on the photocatalytic activity of platinized films. These influences would not only rely on the effects of a post-platinization heat-treatment [40] but also on interactions occurring during the photocatalytic process [41]. Further studies will therefore be necessary to better assess such influences.

## 4. Conclusion

Sol–gel $TiO_2$ thin films have been loaded with platinum clusters through a photo-platinization method using water/ethanol platinum solutions. FEG-SEM, FTIR, and XPS characterizations show that the water/ethanol composition of the platinum solution and temperature of the post-platinization heat-treatment strongly influence the size and distribution of platinum clusters as well as the surface chemical state of platinized film. In particular, ethanol rich solutions induce adsorption of CO at the surface of Pt clusters and total desorption of CO requires a heat-treatment at 400 °C or more. Conversely, platinization in the presence of a water excess reduces the CO contamination and seems to promote water adsorption at the surface of Pt clusters. This study suggests that the nature and amount of species adsorbed at the Pt surface as well as the amount of loaded platinum are important parameters that govern the photocatalytic activity of platinized films. Photocatalytic reactions induced by platinized films follow bi-regime kinetics. The first regime is characterized by a rather high initial rate constant $k_1$, while long term UV exposition promotes a more or less pronounced deceleration of the photocatalytic reaction yielding a weaker rate constant $k_2$. Deceleration in the second photocatalysis regime is attributed to a reduced transfer of photo-generated electrons from platinum clusters to dissolved oxygen, which promotes an enhanced $e^-/p^+$ recombination. Best photocatalytic activities are measured for films platinized from a water rich Pt solution. In these conditions, the absence of any Pt contamination by CO would promote a better transfer of photo-electrons, while the presence of adsorbed water at the Pt clusters might induce a greater amount of active $OH^0$ radicals. Both features conjointly yield a greater photocatalytic activity that is characterized by an optimal initial rate constant and an efficient reduction of the deceleration in the second photocatalysis regime. Photo-activity improvement is completed by a suitable adjustment of the platinization duration, which determines an optimal amount of Pt clusters, and post-platinization temperature, which promotes a partial desorption of adsorbed carbonated species. Consequently, in this study, optimal photocatalytic activities required a platinization for about 90–120 min in presence of a water excess, followed by a heat-treatment in the 250–400 °C thermal range. Films processed in such conditions exhibited $k_1$ and $k_2$ rate constants which were four times and three times greater, respectively, than the rate constant measured for non-platinized films. New studies will be necessary to better understand photocatalytic properties of platinized films and to assess influences of additional parameters or mechanisms, including the effects of size and distribution of platinum particles or the effects of platinum-support interactions.

## References


[1] A.J. Nozik, Appl. Phys. Lett. 30 (1977) 567.
[2] T. Sakata, T. Kawai, K. Hashimoto, Chem. Phys. Lett. 88 (1) (1982) 50.
[3] B. Ohtani, K. Iwai, S.-I. Nishimoto, S. Sato, J. Phys. Chem. B 101 (1997) 3349.
[4] M. Sadeghi, W. Liu, T.-G. Zhang, P. Stavropoulos, B. Levy, J. Phys. Chem. 100 (1996) 19466.
[5] S. Gan, Y. Liang, D.R. Baer, M.R. Sievers, G.S. Herman, C.H.F. Peden, J. Phys. Chem. B 105 (2001) 2412.
[6] K.T. Ranjit, B. Viswanathan, J. Photochem. Photobiol. A: Chem. 108 (1997) 73.
[7] J.C. Kennedy III, A.K. Datye, J. Catal. 179 (1998) 375.
[8] A. Yamakata, T. Ishibashi, H. Onishi, J. Phys. Chem. B 105 (2001) 7258.
[9] U. Siemon, D. Bahnemann, J.J. Testa, D. Rodriguez, M.I. Litter, N. Bruno, J. Photochem. Photobiol. A: Chem. 148 (2002) 247.
[10] J.M. Herrmann, J. Disdier, P. Pichat, A. Fernandez, A. Gonzalez-Elipe, G. Munuera, C. Leclercq, J. Catal. 132 (1991) 490.
[11] O. Carp, C.L. Huisman, A. Reller, Prog. Sol. State Chem. 32 (2004) 33.
[12] A. Fernandez, G. Lassaletta, V.M. Jimenez, A. Justo, A.R. Gonzalez-Elipe, J.M. Herrmann, H. Tahiri, Y. Ait-Ichou, Appl. Catal. B: Environ. 7 (1995) 49.
[13] J.C. Yu, W. Ho, J. Lin, H. Yip, P.K. Wong, Environ. Sci. Technol. 37 (2003) 2296.
[14] V. Roméas, P. Pichat, C. Guillard, T. Chopin, C. Lehaut, Ind. Eng. Chem. Res. 38 (1999) 3878.
[15] A. Mills, A. Lepre, N. Elliott, S. Bhopal, I.P. Parkin, S.A. O'Neill, J. Photochem. Photobiol. A: Chem. 160 (2003) 213.
[16] M. Zhang, Z. Jin, Z. Zhang, H. Dang, Appl. Surf. Sci. 250 (2005) 29.
[17] M. Zhang, Z. Jin, J. Zhang, Z. Zhang, H. Dang, J. Mol. Catal. A: Chem. 225 (2005) 59.
[18] C. He, Y. Xiong, X. Zhu, X. Li, Appl. Catal. A: Gen. 275 (2004) 55.
[19] S.C. Kim, M.C. Heo, S.H. Hahn, C.W. Lee, J.H. Joo, J.S. Kim, I.K. Yoo, E.J. Kim, Mater. Lett. 59 (2005) 2059.
[20] M. Langlet, A. Kim, M. Audier, C. Guillard, J.M. Herrmann, J. Mater. Sci. 38 (2003) 3945.
[21] M. Fallet, S. Permpoon, J.L. Deschanvres, M. Langlet, J. Mater. Sci. 41 (10) (2006) 291.
[22] M. Langlet, S. Permpoon, D. Riassetto, G. Berthomé, E. Pernot, J.C. Joud, J. Photochem. Photobiol. A: Chem. 181 (2–3) (2006) 203.
[23] K.S. Kim, N. Winograd, R.E. Davis, J. Am. Chem. Soc. 92 (23) (1971) 6296.
[24] T.L. Barr, J. Phys. Chem. 82 (16) (1978) 1801.
[25] Z. Liu, B. Guo, L. Hang, H. Jiang, J. Photochem. Photobiol. A: Chem. 172 (2005) 81.
[26] S. Zafeiratos, G. Papakonstantinou, M.M. Jacksic, S.G. Neophytides, J. Catal. 232 (2005) 127.

[27] G. Facchin, G. Carturan, R. Campostrini, S. Gianella, L. Lutterotti, L. Armelao, G. Marci, L. Palmisano, A. Sclafani, J. Sol–Gel Sci. Tech. 18 (2000) 29.
[28] R.J. Gonzalez, R. Zallen, H. Berger, Phys. Rev. B 55 (11) (1997) 7014.
[29] L.V. Mattos, F.B. Noronha, J. Catal. 233 (2005) 453.
[30] T. Sakata, T. Kawai, Chem. Phys. Lett. 80 (2) (1981) 341.
[31] M.L. Sauer, D.F. Ollis, J. Catal. 158 (1996) 570.
[32] M. Burgos, M. Langlet, Thin Solid Films 349 (1999) 19.
[33] J.R.S. Brownson, M.I. Tejedor-Tejedor, M.A. Anderson, J. Phys. Chem. B 110 (2006) 12494.
[34] A. Yee, S.J. Morrison, H. Idriss, J. Catal. 191 (2000) 30.
[35] G. Busca, V. Lorenzelli, Mater. Chem. 7 (1982) 89.
[36] H. Idriss, C. Diagne, J.P. Hindermann, A. Kiennemann, M.A. Barteau, J. Catal. 155 (1995) 219.
[37] J.M. Herrmann, Catal. Today 53 (1999) 115.
[38] H. Lachheb, E. Puzenat, A. Houas, M. Ksibi, E. Elaloui, C. Guillard, J.M. Herrmann, Appl. Catal. B: Environ. 39 (2002) 75.
[39] V. Subramanian, E. Wolf, P.V. Kamat, J. Phys. Chem. B 105 (2001) 11439.
[40] M. Fernandez-Garcia, A. Fuerte, M.D. Hernandez-Alonso, J. Soria, A. Martinez-Arias, J. Catal. 245 (2007) 84.
[41] D. Lahiri, V. Subramanian, B.A. Bunker, P.V. Kamat, J. Chem. Phys. 124 (2006) 204720.